Behaviors of ionization wave packets within finite positive columns

K. Ohe and T. Kimura
Department of Systems Engineering, Nagoya Institute of Technology, Gokiso-cho, Showa-ku, Nagoya 466, Japan

(Received 9 July 1991; accepted for publication 11 September 1991)

Behavior of ionization wave packets was investigated in wave-free positive columns of Ne-N_2 and He. The position of envelope wave packet launching was displaced with an excitor along the tube axis, while phases of included carrier waves shifted only a little. The anode end of positive column played an important role in propagation of the carrier wave, causing such a phase shift. The influence of anode end on the wave behavior was explained by a phenomenological model.

I. INTRODUCTION

Ionization waves are excited in positive columns with fluctuating optical radiation intensities closely related to fluctuations in ionization.[1] Observations of ionization wave packet with a small amplitude excited in a wave-free positive column have greatly contributed to establish the linear theory.[2] The wave packet evolved was little dependent of applied waveforms to excite, such as a rectangular, a sinusoidal burst, and δ-function-like ones,[3] in contrast to dispersive plasma waves in which waveforms evolved depended on initial perturbations; for example, ion-acoustic-wave trains that evolved from a δ-function pulse had an Airy function waveform.[4]

A phenomenological analysis using the Fourier integral[5,6] showed that a wave packet with a coherent carrier wave was evolved from an initial δ-function perturbation under an assumption that the wave was able to grow with only a narrow band of wave number. The evolution of the wave packet from a small Gaussian perturbation was also simulated by numerically calculating a set of hydrodynamic equations.[7] These analyses were performed by assuming that the wave packet excited at a position, where the perturbation was applied, propagated over an infinite positive column. So far, there have been a few observations to identify the position of the wave packet launching, in which the position is in the neighborhood of application of the initial pulse,[8] but still retaining some ambiguities. Concerning experiments of the wave packet propagation, no account has been taken of the finite length of the column, which may play an important role. As is well known, ionization waves excited in inert gases are backward ones whose group velocity is toward the anode, opposing to the phase velocity. The position of the wave phase launching may be affected by the finite length for such a backward wave, because the phase propagates toward the cathode from the anode.

In the present paper, we describe experiments associated with the excitation of ionization wave packets using an excitor movable along the tube axis in wave-free positive columns of He and Ne-N_2. The behavior of wave packets influenced by the anode end is analyzed by a phenomenological model modifying that used by Rutscher and Wojaczek,[6] and compared with the experimental results.

II. EXPERIMENT AND RESULTS

The following notations are used:

P, the gas pressure

I_d, the discharge current

d, the spatial growth rate

ψ, the temporal growth rate

ψ_1, the temporal growth rate corresponding to the maximum d

V_g, V_p, the group and phase velocities, respectively

x_{ex}, the displacement of excitor

t_B, the time at which the packet reaches its maximum

x_0, the position of wave packet launching

x_p, the phase shift of wave crest

T, the period of the frequency of applied burst voltage

$S(x,t)$, the wave packet

$H(x,t)$, the envelope of wave packet

C, constant

k_1, the wave number at ψ_1

ω_1, the frequency at ψ_1

x_a, the position of anode end

t_1, the onset time of the wave packet at x_a

x_1, the resonance length of wave packet

T_1, the resonance time corresponding to x_1

L, the distance between x_{ex} and x_a

l, the distance that a wave launched at x_a can propagate

n, the number of temporal carrier waves included in the packet

m, the number of spatial carrier waves included in the packet

x_b, the position monitoring simulated waves.

A schematic diagram of the experimental apparatus is shown in Fig. 1. The glass discharge tube with 6.5 cm inner diameter and 113 cm length was used in the experiment, filled with Ne-N_2 mixed gas, whose mixing ratio was 13–3 at $p = 0.4$ Torr, and with He at $p = 0.28$ Torr. Both positive columns operated by $I_d = 150$ mA in Ne-N_2 and $I_d = 200$ mA in He were kept wave-free. The ionization wave damped gradually toward the anode with $d = -0.026$ cm^{-1} in the former, while the wave grew slightly with $d = 0.05$ cm^{-1} in the latter. A wave packet was excited by applying a sinusoidal burst voltage of one cycle with frequencies from 2 to 50 kHz periodically repeating with a frequency of 100 Hz to a circular excitor,

 0021-8979/91/127282-07$03.00

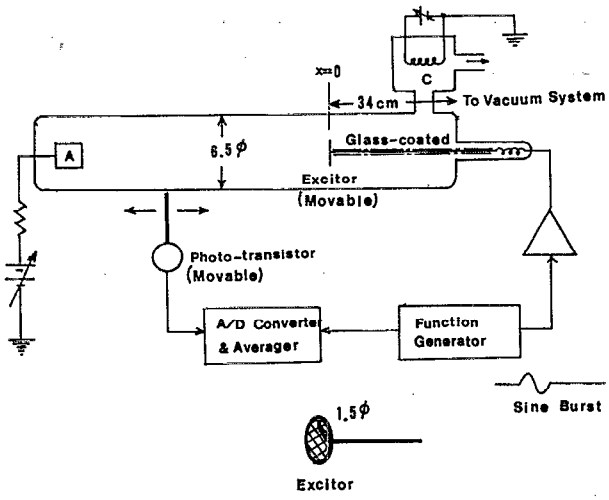

FIG. 1. Schematic diagram of experimental apparatus.

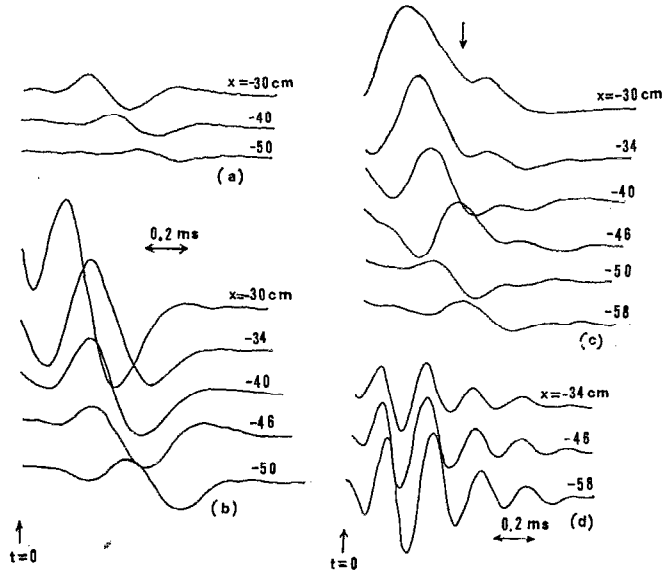

FIG. 2. Typical wave patterns of wave packet. The wave packets excited in Ne-N_2 are shown in (a), (b), and (c), and that excited in He in (d). (a) and (d) are for $x_{ex} = 0$, while x_{ex} is at -5 cm in (b) and -7.5 cm in (c).

which was made of tungsten mesh with 1.5 cm diameter, movable along the tube axis between 34 and 58 cm from the cathode. The fluctuation related to the wave packet was optically detected through a slit-phototransistor movable along the tube axis. The detected signals were digitized

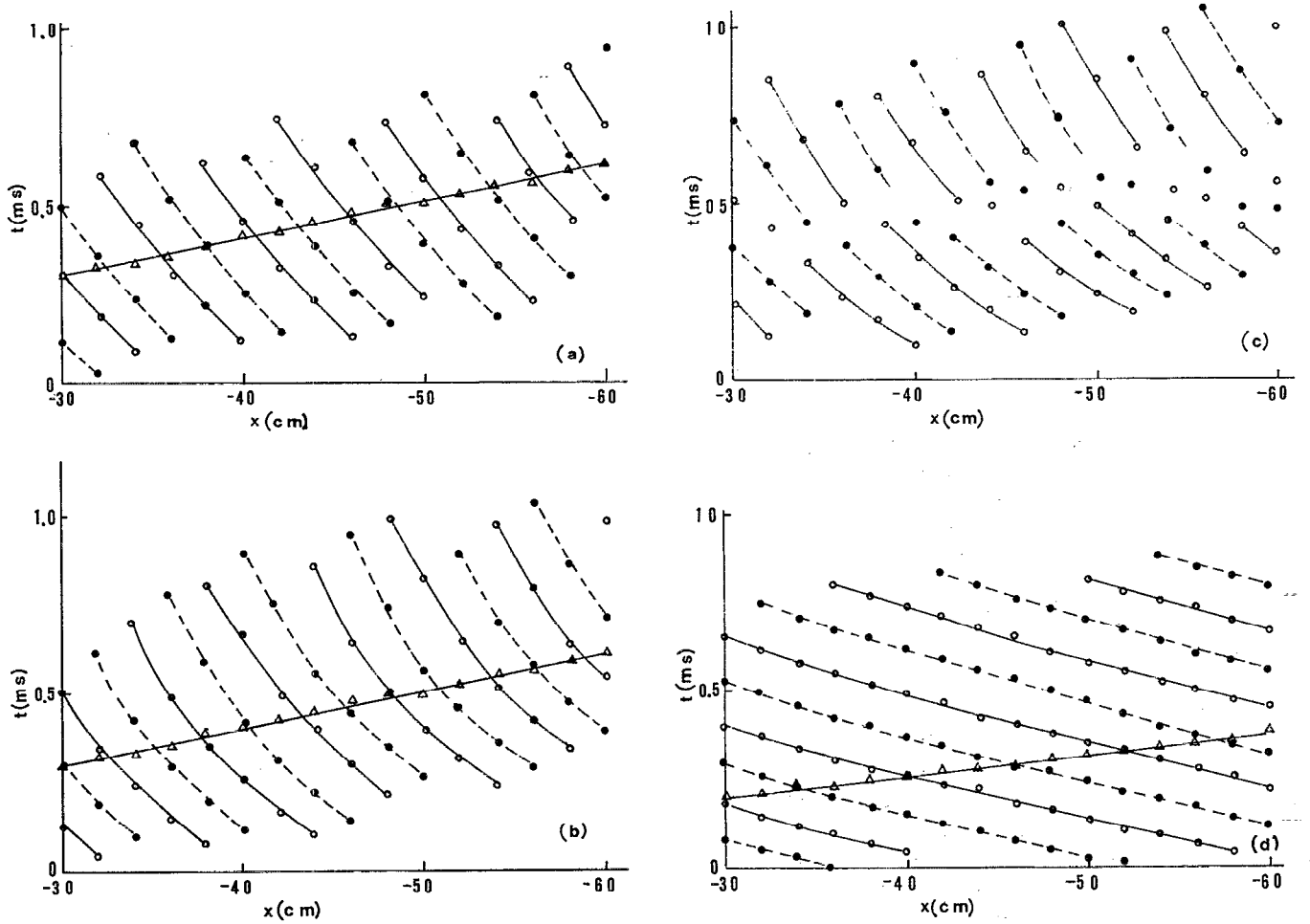

FIG. 3. (t,x) diagrams of t_B (△), wave crest (○), and wave-trough (●). (a)–(d) correspond to (a)–(d) in Fig. 2, respectively.

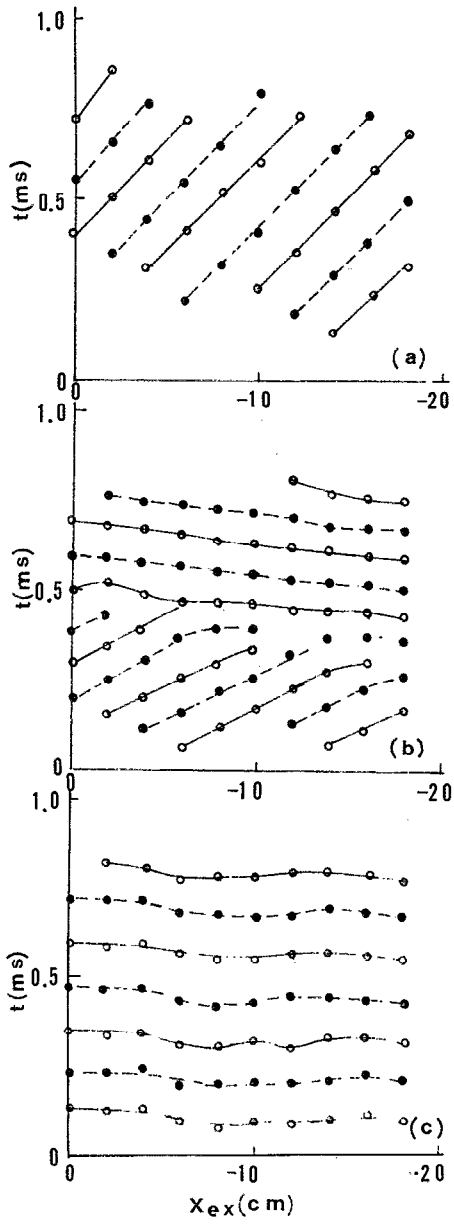

FIG. 4. Phase shifts of wave crest (○) and trough (●), observed at $x = -50$ cm, vs x_{ex} for Ne-N_2 in (a) and (b), and that for He in (c). The envelope H damped out at the anode end in (a) but remained in (b) and (c), where H was smaller in (b) than in (c).

with a sampling width of 2.44 μs and averaged 32 times to improve the signal-to-noise ratio.

Some typical wave patterns detected at various x are shown in Figs. 2(a)–2(d), in which 2(a)–2(c) are for Ne-N_2 and 2(d) for He. The position x appeared to be 34 cm from the cathode end of the tube. Figure 2(a) shows some wave patterns of an extremely small wave packet which damps out near the anode, where the ratio of the maximum amplitude of the wave packet to the steady-state, ac/dc detected at $x = -50$ cm is 0.034%. On the other hand, patterns of slightly larger packet, of which a small amplitude still remains near the anode end, are shown in 2(b) and 2(c), where ac/dc is 0.15%. No distortion in waveform was included in 2(a), 2(b), and 2(d) except for 2(c), in which a distortion appeared after a time shown by an arrow, despite of application of the same burst voltage as those of 2(b) and 2(c). The difference in waveform may be caused by the influence of the anode end, as will be discussed later. Although a finite amplitude remained at the anode end in 2(d), no distortion appeared in the patterns, where ac/dc was 2.2%. All of these wave packets can be classified in the linear scheme, because of their small wave amplitude.

Figures 3(a)–3(d) show (t,x) diagrams of t_B, of which slope correspond to V_g, and those of wave crest and trough, of which slope at t_B is V_p.[5,6] The diagrams shown in 3(a), 3(b), and 3(c) are for the packet in Ne-N_2 and that shown in 3(d) for He, respectively. The values of V_p and V_g were 1.82×10^4 cm/s and -8.51×10^4 cm/s for the former and 7.7×10^4 cm/s and -2.2×10^5 cm/s for the latter, keeping respective constant values throughout the column. The wavelength λ was 6.5 cm for the wave in Ne-N_2 and 17.3 cm for He. A distortion included in 3(c) depended on the excitor position as follows. The wave crest and trough observed at $x = -50$ cm shifted with x_{ex}, as is shown in Figs. 4(a)–4(c), where 4(a) and 4(b) correspond to the packet in Ne-N_2 and 4(c) to He. The phases of wave crest and trough delayed with x_{ex} in 4(a), contrasting to slight phase precedence in 4(c). If the packet propagated over the finite column, all of the phase delays would be the same as that in 4(a), because of no influence of the column end on the phase, as is discussed in the Sec. II. In practice, however, the finite column length induced a large difference in phase delay between 4(a) and 4(c), since the packet damped out in 4(a), whereas the packet still remained in 4(c), eventually yielding some distortions in wave patterns caused by superimposing the waves with and without the influence of the anode end. The extrapo-

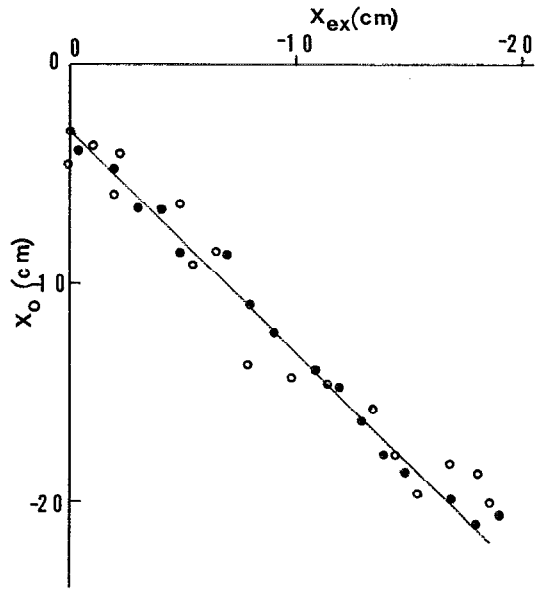

FIG. 5. Position x_0 vs x_{ex}, where (●) is for Ne-N_2 and (○) for He.

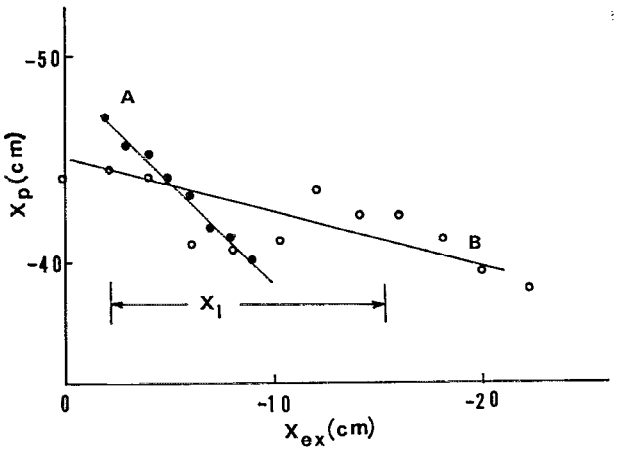

FIG. 6. Phase-shift x_p of a certain wave crest with x_{ex}. Relationship between x_p and x_{ex}, which is indicated by A, is free from the influence of the anode end, whereas that for He, which is indicated by B, is influenced by the end. The linear line indicated by B was calculated from Eq. (7).

lated (t,x) diagram of t_B intersected with the x axis at x_0, from which x_0 can be determined. A direct proportion between x_0 and x_{ex} obtained for all cases showed no influence of the anode end, as is shown in Fig. 5. The relation between x_{ex} and x_p of a wave crest for certain fixed time t is shown in Fig. 6. Deviation from a linear line indicated by B resulted from the influence of the anode end, contrasting to a linear one indicated by A, in which the end had no influence because the wave damped out. Despite the application of the same burst voltage, the wave packet excited varied periodically with x_{ex} as indicated by B, in contrast to a monotonously exponential increase by A, as is shown in Fig. 7. The exponential increase resulted in no influence of

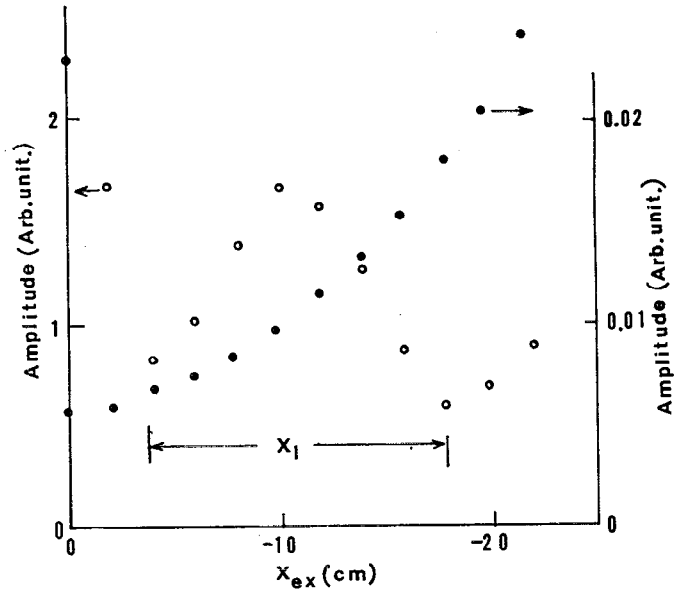

FIG. 7. Amplitude dependence of H, observed at $x=-40$ cm, on x_{ex}. The dependence shown by (○) is for He and that by (●) for Ne-N_2. The resonance length x_1 was calculated by Eq. (6).

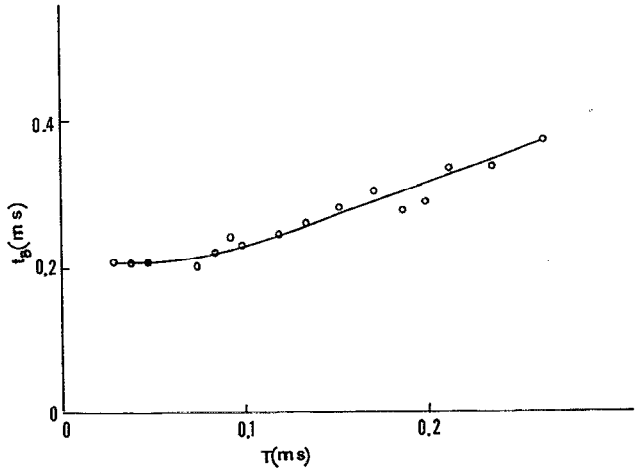

FIG. 8. Typical dependence of t_B on T observed at $x=-50$ cm for He.

the end where the wave damped out, while the periodic variation resulted from the influence of the end.

A typical dependence of t_B on T was observed for He at $x=-50$ cm, as shown in Fig. 8. The time t_B decreased gradually with decreasing T, being constant for T smaller than 8×10^{-5} s. The relation between x_0 and x_{ex} shown in Fig. 5 was measured for such a small T in order to avoid the ambiguity depending on T.

III. PHENOMENOLOGICAL DESCRIPTION OF WAVE PACKET PROPAGATION WITHIN FINITE COLUMN

A. Wave packet

A wave packet $S(x,t)$ evolved from an initial δ-function perturbation is expressed by using the Fourier integral,[5,6]

$$S(x,t)=H(x,t)\cos\ \Phi(x,t). \tag{1}$$

The envelope $H(x,t)$, and its carrier waves $\cos\Phi(x,t)$ are expressed as

$$H(x,t)=C(4\pi|B|t)^{-1/2}\times\exp[-(x-\omega_1't)^2/(4b_1t)-dx], \tag{2}$$

$$\Phi(x,t)=k_1x-\omega_1t+(x-\omega_1't)^2/(4q_1t)-\Psi/2, \tag{3}$$

where $B=1/2(\omega_1''^2+\psi_1''^2)^{1/2}$, $\Psi=\tan^{-1}(-\omega_1''/\psi_1'')$, $b_1=-(\omega_1''^2+\psi_1''^2)/(2\psi_1'')$, $q_1=(\omega_1''^2+\psi_1''^2)/(2\omega_1'')$. The growth rate $\psi(k)$ can be assumed to be a quadratic form with the sharp maximum around $k-k_1$. This assumption enables us to expand $\omega(k)$ around $k-k_1$ as follows:

$$\omega(k)-\omega_1+\omega_1'(k-k_1)+1/2\omega_1''(k-k_1)^2, \tag{4a}$$

$$\psi(k)=\psi_1+1/2\psi_1''(k-k_1)^2, \tag{4b}$$

where $\omega_1'\equiv V_g$. Numerical values to calculate Eqs. (2) and (3) were obtained from a dispersion relation for Ne-N_2 detected by a conventional interferometric system using a lock-in amplifier,[9] as is shown in Fig. 9.

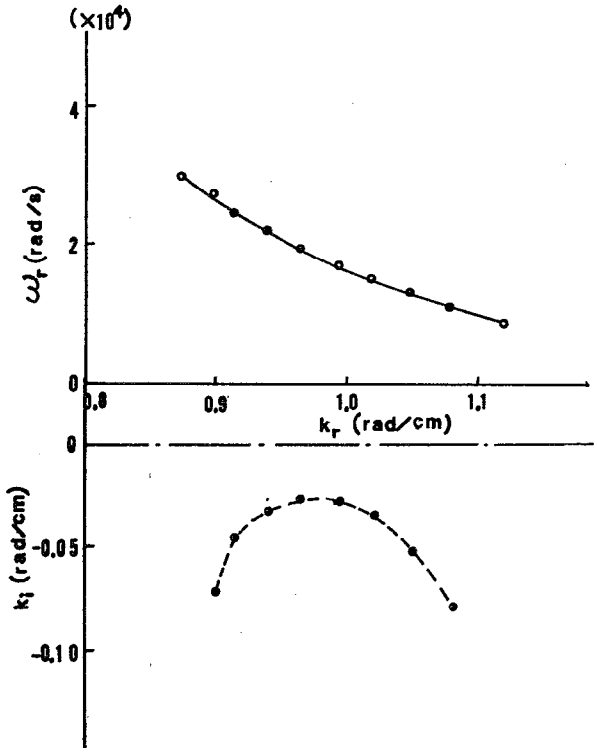

FIG. 9. Observed dispersion relation of the ionization wave for Ne-N_2.

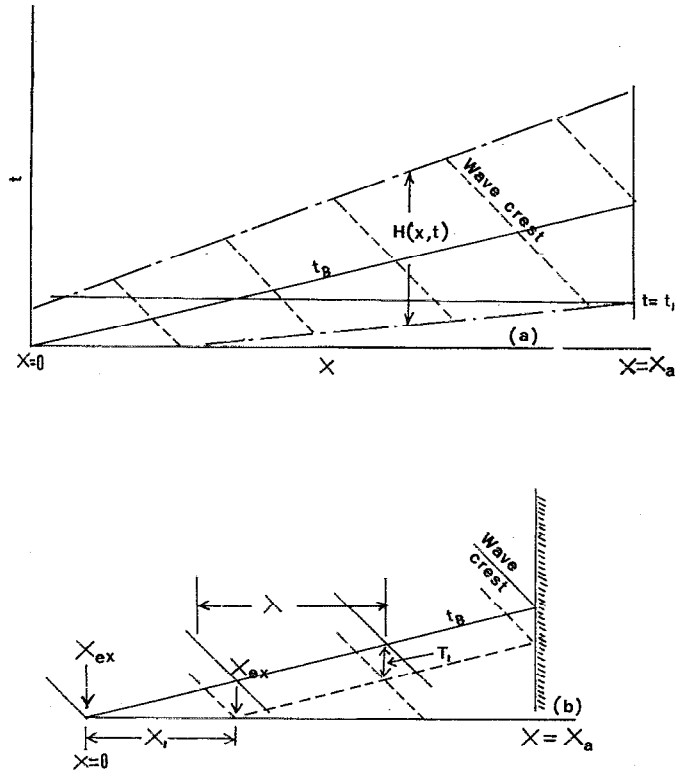

FIG. 10. (a) Schematic (t,x) diagrams of t_B and wave phase $\Phi=2\pi n'$, where n' is an integer. We assume here as follows: (1) the anode end is $x = x_a$, there expressing $H(x_a,t)$, (2) the ratio of V_g to V_p is 3, and (3) $\Phi(x,t)$ is $k_1(x-\omega_1)t$. (b) Shifts of t_B and wave phase from solid to dotted lines with x_{ex} from $x=0$ to x_1. For simplicity, the line of t_B is assumed to intersect with one of the wave crests at $x=0$ as well as $x=x_a$.

B. Wave packet propagation through finite positive column

If a wave packet propagates through a finite column, Eq. (1) must be modified by taking account of the anode end of the column. Assuming that $S(x,t)$ excited at $x=0$ propagates through the finite column toward x_a, the envelope $H(x,t)$ propagates toward x_a, while the phase $\cos\Phi(x,t)$ propagates toward $x=0$ as shown in Fig. 10(a), where $\Phi(x,t)$ is approximated as $k_1x-\omega_1t$, for simplicity. In other words, the wave phase $\cos\Phi$ launched at $x = x_a$ would propagate along x toward the cathode through a channel developed by H. However, the law of cause and effect would permit the wave phase to propagate only after t_1 which is determined by duration of $H(x_a,t)$ at $x = x_a$. This argument leads to a wave excitation mechanism that a wave phase without the influence of anode end can evolve in a duration from $t=0$ to t_1, while after $t=t_1$ a wave superimposed by two waves with and without the influence evolves as follows:

$$S(x,t)=H(x,t)\cos\Phi(x,t) \quad \text{for } 0\leqslant t<t_1, \tag{5a}$$

$$S(x,t)=\tfrac{1}{2}[H(-x_a-x,t)\cos\Phi(-x,t) + H(x,t)\cos\Phi(x,t)] \quad \text{for } t_1\leqslant t. \tag{5b}$$

Taking account of the slope of the dispersion relation, q_1 should be replaced by $-q_1$ in $\Phi(-x,t)$.

C. Wave packet behavior depending on excitor position

When the excitor position displaces from $x=0$ to x_{ex}, a wave packet excited at $x = x_{ex}$ can be expressed by $S(x - x_{ex},t)$ for the infinite column. On the other hand, in the finite column $S(x,t)$ should be also modified as $S(x - x_{ex},t)$ in Eqs. (5a) and (5b), and t should be replaced by $t + t_{ex}$ in the first term of the right hand in Eq. (5b), where t_{ex} is obtained by $t_{ex} = x_{ex}/V_g$. If a forward wave with λ would be excited in L, the wave would be resonant under the condition of $L=m'\lambda$, where m' is the integer, thus yielding a resonance length equal to λ. The resonance length x_1 shown in Fig. 7 was, however, slightly shorter than λ. The length x_1 may be explained from the backward wave property and the influence of the anode end as follows: Let us assume that the envelope H excited at $x_{ex} = 0$ is in a resonance and four wave crests are included in L, as represented by solid lines in (t,x) diagrams in Fig. 10(b). The next resonance may occur at $x_{ex} = -x_1$, in which three wave crests are included, as represented by solid lines, because x_a is fixed. Thus the length x_1 depends on the slopes of t_B and the wave crests, in other words, it is proportional to the ratio of V_g to V_p as follows:

$$x_1=|V_g|\lambda/(|V_g|+V_p). \tag{6}$$

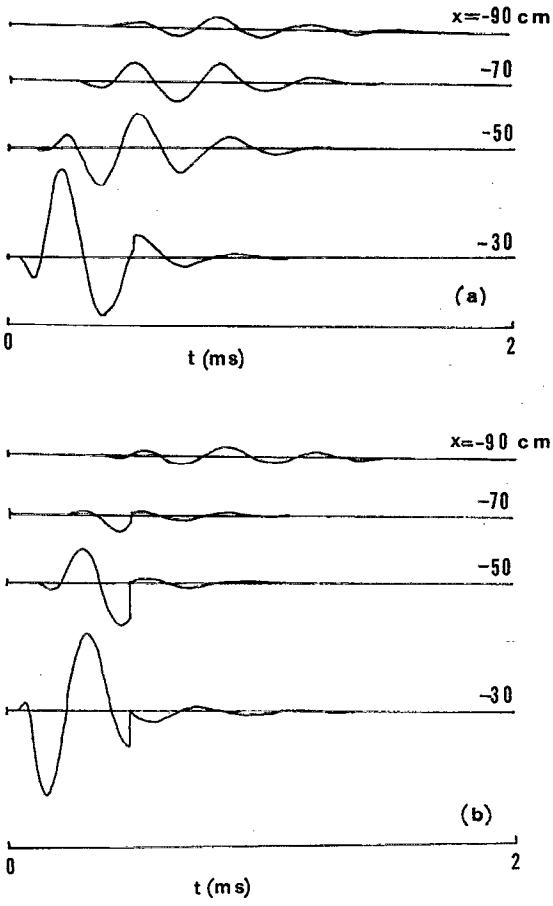

FIG. 11. Typical wave patterns simulated by numerically calculating Eqs. (5a) and (5b). The wave patterns for $x_{ex} = -2$ cm are shown in (a) and those for -4 cm in (b).

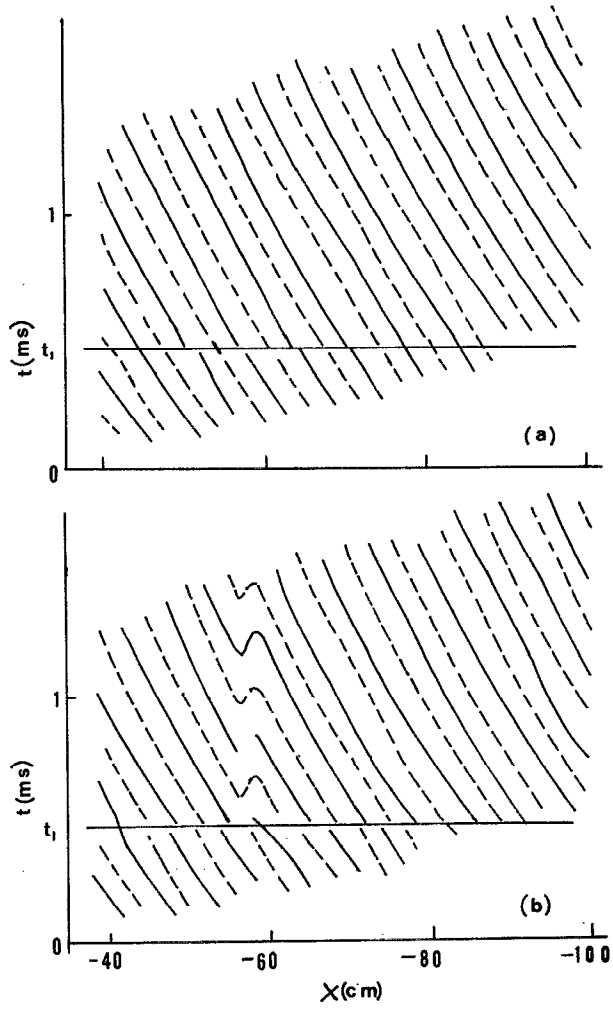

FIG. 12. Simulated (x,t) diagrams of wave crest (solid lines) and trough (dotted lines), where (a) is for $x_{ex} = -2$ cm and (b) for $x_{ex} = -4$ cm.

The above argument leads to one to deduce the dependence of x_p on x_{ex} for the finite column as follows:

$$x_p = V_p x_{ex}/(|V_g| + V_p). \tag{7}$$

IV. SIMULATION AND DISCUSSION

The propagation of the wave packet through a finite column is simulated by numerically calculating Eqs. (5a) and (5b) under the following assumption: (1) The column length is 100 cm ($x_a = 100$ cm). (2) The constant C in Eq. (1) is 10, by which the initial amplitude of H is determined. (3) d is -0.025 cm^{-1} (rad/s). (4) The influence of the anode end occurs with H larger than 10^{-3}, which eventually determines t_1. In order to determine the time width of H at x_a, the value is used, thus having no physical meaning. Further experiments are necessary to obtain the actual width.

Figures 11(a) and 11(b) show some wave patterns of wave packets for $x_{ex} = -2$ and -4 cm, respectively. Only a small distortion was included in (a), because $\Phi(x - x_{ext},t)$ was approximately in phase with $\Phi(-x,t)$, while there was a large distortion in (b) caused by a large phase difference between them. The simulated wave packets shown in Figs. 11(a) and 11(b) may correspond to the experimental results shown in Figs. 2(b) and 2(c), respectively. Displacement of the excitor from $x_{ex} = -2$ to -4 cm, for example, corresponded to a phase difference of 0.61 π. Sharp discontinuities which appeared in simulated waveforms as shown in Fig. 11(b) were not observed in the experiment. The high-frequency components corresponding to the discontinuity may damp out, because only a few waves with a narrow frequency component around ω_1 can propagate through the positive column as shown in Fig. 9, thus covering such a sharp discontinuity in the experiment. In order to clarify the discontinuity further, two (t,x) diagrams of wave crest and trough were calculated, as are shown in Figs. 12(a) and 12(b), in which the numerical values and x_{ex} were the same as those in Figs. 11(a) and 11(b). The (t,x) diagram in 11(a) included only a little phase shift, whereas that in 11(b) included some phase shifts, corresponding to Figs. 3(b) and 3(c), respectively.

It was noticed that a phase shift occurring at $t = t_1$ had an influence on waveforms even later than t_1, resulting in curvature of (t,x) diagram in wave crest caused by the curvature in dispersion relation. The wave launched at x_a propagates over l toward the cathode with disturbing the waveform. Thus it is important to estimate l, which may be evaluated as $l = m\lambda$. Since $m/n \doteqdot |V_g|/V_p$, which has been

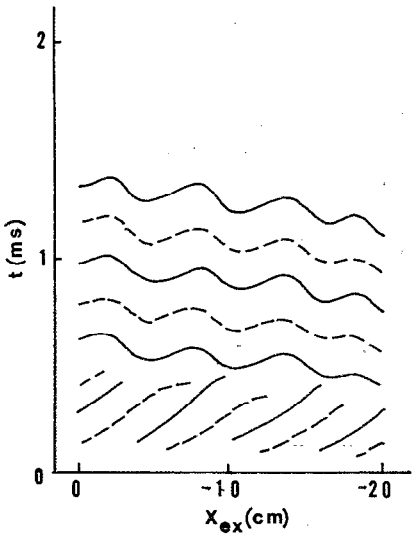

FIG. 13. Simulated (x_{ex},t) diagrams of wave crest (solid lines) and trough (dotted lines) at $x=-50$ cm as a function of x_{ex}.

deduced in a previous paper,[10] the distance l can be easily evaluated by measuring n. The distance l for the case of Fig. 2(b) was 30.4 cm. This argument shows that the anode end has influence over a long length of the column, requiring to take account of it in ionization wave experiments.

The phase shift depending on x_{ex} appearing at $x = x_b$ was simulated by calculating Eqs. (5a) and (5b) as a function of x_{ex} and t, after replacing $S(x,t)$ with $S(x_b - x_{ex},t)$, as is shown in Fig. 13, where the numerical values for the wave in Ne-N_2 and $x_b = -50$ cm were used. A drastic change of the (t,x_{ex}) diagram at $t=t_1$ agreed well with the experimentals except for a result that t_1 experimentally observed was slightly later than the simulated one. A periodic fluctuation appearing in the simulated diagram was not observed in the experiment, since in practice, the column length in which a wave with λ propagates may be somewhat adjustable so as to be $N\lambda$, where N is integer. From the direct proportion between x_0 and x_{ex} shown in Fig. 5, the envelope $H(x,t)$ is little influenced by the anode end. Identification of the position of the wave packet launching by the time flight of t_B is appropriate, despite the ambiguity due to the scattered plots of experimental results. The position was about 3 cm toward the anode from the excitor as shown in Fig. 5. The relation of direct proportion between x_p and x_{ex} indicated by A for Ne-N_2 shown in Fig. 6 was an evidence of the wave packet launching near the excitor as well. No influence of the anode end due to the damped-out wave yielded such a relation, while the experimental plots for He agreed with Eq. (7), where the wave remained. The influence caused a periodic scattering of experimental plots around the line with the gradient $V_p/(|V_g| + V_p) = 0.36$. The scattering was attributed to the periodic resonance in amplitude of the excited wave packet as expressed by Eq. (6). The resonance length 14 cm calculated for the wave in He agreed well with x_1 shown in Fig. 7. Such a resonance affected the experimental (t,x_{ex}) diagrams as well as the simulated one, as shown in Figs. 4 and 13, respectively.

In order for Eq. (1) to be applicable, the initial perturbation must be the δ function. No dependence of t_B on T smaller than 8×10^{-5} s for He shown in Fig. 7 confirmed that such a short sinusoidal burst was regarded as the δ-function perturbation.

V. SUMMARY

Propagation of ionization waves within a finite positive column was investigated by exciting a small wave packet using an excitor movable along the tube axis in wave-free columns of Ne-N_2 and He. Behaviors of the wave packet were simulated by numerically calculating an equation describing the packet by taking account of the influence of the anode end. Results obtained are summarized as follows.

(1) The envelope of the wave packet launched near the excitor propagated toward the anode with little influence of the anode end. Then the position of envelope launching was displaced with the excitor. The wave phases were also shifted with the excitor in a manner similar to that of the envelope when it damped out at the end, while the phase shifts were much smaller, whenever the envelope remained there. The influence of anode end caused the phase shift was determined by x_{ex}/V_g.

(2) Carrier waves without the influence of the anode end evolved and propagated toward the cathode before a certain time when the envelope arrived at the end. On the other hand, the wave superimposed by two waves with and without the influence propagated after the time, causing some distortions on waveform.

(3) The anode end caused a resonance in amplitude of the excited envelope, which was slightly shorter than the wavelength. The resonance length was determined by dividing the wavelength in a ratio proportional to the group and phase velocities.

ACKNOWLEDGMENTS

The authors would like to thank M. Mori of Nagoya University for fabrication of the discharge tube. They are also indebted to M. Shimoide and S. Koma for their assistance with the numerical calculations.

[1] N. L. Oleson and A. W. Cooper, Adv. Electron. Electron Phys. **24**, 155 (1968).
[2] L. Pekarek and V. Krejci, Czech. J. Phys. B **12**, 296 (1962).
[3] L. Pekarek, Czech. J. Phys. **9**, 67 (1959).
[4] G. B. Witham, *Linear and Nonlinear Waves* (Wiley, New York, 1974).
[5] N. L. Oleson and A. W. Cooper, Adv. Electron. Electron Phys. **24**, 225 (1968).
[6] A. Rutscher and K. Wojaczek, Beitr. Plasmaphys. **2**, 122 (1962).
[7] I. Grabec, Phys. Fluids **17**, 1834 (1974).
[8] M. Novak and K. Wojaczek, Beitr. Plasmaphys. **2**, 66 (1962).
[9] For example, A. J. Duncan, J. R. Forrest, F. W. Crawford, and S. A. Self, Phys. Fluids **12**, 2607 (1969).
[10] K. Ohe, K. Asano, and S. Takeda, J. Phys. Soc. Jpn. **49**, 350 (1980).